Optimization of the synthesis and operational parameters for NOM removal with response surface methodology during nano-composite membrane filtration

Nader Yousefi, Ramin Nabizadeh, Simin Nasseri, Mehdi Khoobi, Shahrokh Nazmara and Amir Hossein Mahvi

ABSTRACT

The aim of this study was to investigate membrane synthesis by interfacial polymerization methods, the application of synthesized nano-composite membrane for natural organic matters (NOMs) removal from water, evaluation of fouling mechanism and antifouling properties. Polysulfone (PSf) was selected as a porous ultrafiltration membrane support and interfacial polymerization was done using tannic acid (TA) and Trimesoyl chloride (TMC) with central composite design (CCD). The effects of TA and TMC monomer concentrations, reaction time and post treatment temperature was evaluated. The synthesized membrane was characterized by field emission scanning electron microscope (FESEM), atomic force microscopy (AFM), attenuated total reflection Fourier transform infrared spectroscopy (ATR-FTIR) and water contact angle. Based on the results, the optimum conditions for synthesizing nano-composite were: TA concentration of 0.27 g/L, TMC concentration of 0.22 g/L, reaction time of 68.29 min and temperature of 25.23 °C. The predicted optimum operational conditions were a NOM concentration of 6.429 mg/L; time of 10.931 min and applied pressure of 1.039 bar. The potential applications of the synthesized nano-composite membranes with interfacial polymerization can enhance water treatment.

Key words | disinfection by-product, interfacial polymerization, membrane filtration, nano-composite, response surface methodology

Nader Yousefi
Ramin Nabizadeh
Simin Nasseri
Shahrokh Nazmara
Amir Hossein Mahvi (corresponding author)
Department of Environmental Health Engineering, School of Public Health,
Tehran University of Medical Sciences,
Tehran, Iran
E-mail: *ahmahvi@yahoo.com*

Simin Nasseri
Amir Hossein Mahvi
Center for Water Quality Research (CWQR), Institute for Environmental Research (IER),
Tehran University of Medical Sciences (TUMS),
Tehran, Iran

Mehdi Khoobi
Department of Pharmaceutical Biomaterials and Medical Biomaterials Research Center,
Tehran University of Medical Sciences,
Tehran, Iran
and
Department of Medicinal Chemistry, Faculty of Pharmacy and Pharmaceutical Sciences Research Center,
Tehran University of Medical Sciences,
Tehran, Iran

Amir Hossein Mahvi
Center for Solid Waste Research (CSWR), Institute for Environmental Research (IER),
Tehran University of Medical Sciences (TUMS),
Tehran, Iran
and
National Institute of Health Research,
Tehran University of Medical Sciences,
Tehran, Iran

INTRODUCTION

Natural organic matters (NOMs) are one of the most abundant organic pollutants, so about 50% of dissolved organic materials in rivers are humic substances (Gholami-Borujeni *et al.* 2011a; Jafari *et al.* 2015; Seman *et al.* 2015). NOMs have a direct effect on water quality by reacting with disinfectants and potentially producing harmful disinfectant by-products, as well as indirect effects by impacting water treatment processes, such as reducing the influence of adsorption, and membrane fouling (Yousefi *et al.* 2017).

NOMs may be removed from water resources using coagulation and flocculation, electrocoagulation, adsorption, oxidation (Habuda-Stanić *et al.* 2013; Rezaee *et al.* 2014) and membrane filtration. Many of these processes are generally associated with high energy costs, production of large amounts of sludge and/or wastes, generation of waste brine, formation of intermediate products and high energy consumption. Nanofiltration (NF) membranes, as a novel separation technology, have been widely applied in

doi: 10.2166/wst.2018.037

various industrial and applied fields (Dehghani *et al.* 2008; Mahvi *et al.* 2008; Maleki *et al.* 2010; Malakootian *et al.* 2011, 2015; Shirmardi *et al.* 2012; Wu *et al.* 2013; Yousefi *et al.* 2016). NF has emerged as an attractive process because of high retention of multi-valent ion salts, low operation pressure (Mahvi *et al.* 2009, 2011). The composite membrane prepared by interfacial polymerization is formed over an ultra-thin separating layer on a porous substrate (Li *et al.* 2009; Seman *et al.* 2015). Moreover, the separating layer and porous substrate can be optimized by changing the concentration of monomer in both aqueous and organic phases, reaction temperature and time and monomer ratios (Li *et al.* 2009; Seman *et al.* 2015). Some advantages of thin-film composite membranes prepared by interfacial polymerization are lack of limitation and problems encountered by other membranes formed by the phase inversion method; self-inhibition of reaction; particular function optimization by varying the monomer concentrations and other factors (Seman *et al.* 2015).

The porous support and thin film play an important role in the performance and stability of the membrane. Polysulfone (PSf) has emerged as an attractive polymer for fabricating composite membranes because of its low cost, mechanical stability, resistance to thermal, chemical and biological attacks, ease of processing, appropriate morphology and chemistry, and being widely available (Korikov *et al.* 2006).

The response surface method (RSM) is defined as a statistical method for presenting the relationship between factors and responses and mathematic modelling (Ashrafi *et al.* 2013, 2016). In addition, RSM is used for optimizing physical, chemical and biological experimental processes (Gholami-Borujeni *et al.* 2011b). In this study, RSM was applied to designing the membrane synthesis by interfacial polymerization operational conditions. Since NOM is a most abundant and primary reactant in the formation of trihalomethanes (THMs), the main goal of this research was to investigate membrane synthesis by interfacial polymerization methods and the application of synthesized nano-composite membrane for NOM removal from water.

MATERIALS AND METHODS

Materials

PSf (with average Mw = 22,000 g/mol), piperazine (PIP) and N-N Dimethylformamide (DMF), tannic acid (TA), Trimesoyl chloride (TMC, or 1,3,5-benzenetricarbonyltrichloride) and Triethanolamine (TEOA) was purchased from Sigma-Aldrich Co, USA. Humic acid (HA), bovine serum albumin (BSA), n-hexane, sodium hypochlorite, NaOH, Na_2CO_3 and other inorganic salts were purchased from Merck Company (Germany). All chemicals were analytical grade and used without further purification. The deionized (DI) water was used for the sample preparation and pure water flux measurements.

Analytical methods

The humic acid concentration was determined by UV–Vis spectrophotometer at a maximum adsorption wavelength (Perkin Elmer, lambda 25, USA). A field emission scanning electron microscope (FESEM) (Mira 3 Tescan, Czech Republic) was used for determining the size of the pores and morphology of membrane; the images of membrane were taken at the accelerating voltage of 15 KV. Infra-red (IR) spectra were provided using attenuated total reflectance Fourier transform infrared spectroscopy (ATR-FTIR) spectrometer (Tensor 27, Bruker Inc., Germany). Atomic force microscopy (AFM) (Thermo microscopes Auto probe CP Research, Veeco Instruments, Sunnyvale, CA, USA) was used for top surface morphology and roughness analysis. The contact angle and zeta potential were measured using a water contact angle measurement (OCA 15 Plus, Dataphysics, Germany) and streaming potential method (electro kinetic analyzer (EKA, Anton Paar GmbH, Austria), respectively.

Preparation of composite nanofiltration membranes

Conventional interfacial polymerization method was applied for preparing the composite nanofiltration membranes (Yousefi *et al.* 2017). PSf ultrafiltration membranes were used as the micro-porous support membrane. Pure water flux for PSf ultrafiltration membrane was 130 $L/m^2 \cdot h$ at a pressure of 1 bar and molecular weight cut off of about 50,000. Before the interfacial polymerization reaction, the membrane was hydrophilized with acetone followed by chromic acid solution for 30 min at 65 °C. The detailed fabrication process used as a simple process in this study was carried out as follows. First, a series of aqueous phase solutions were prepared using sodium lauryl sulfate (0.3%, w/v), TEOA (6%, w/v) and variable concentrations of TA (0 to 0.3 wt %) in deionized water. The pH of the aqueous solution was adjusted using a mixture of NaOH and Na_2CO_3, which was mixed in 1:2 proportion. The organic phase solution was prepared by dissolving variable concentrations of TMC (0 to 0.3 wt %) in n-hexane. Before using the PSf as a porous

membrane, it was washed and soaked in water for 24 hours. PSf membranes were immersed in the organic solutions for about 30 min. The PSf saturated with TMC was soaked in the TA (aqueous solution) for 35 min to diffuse the TA into the porous support and then the excess solution of the organic phase was drained off from a membrane surface with filter papers. In a later step, the saturated membrane was immersed in the TMC (organic phase) to ensure that the polymerization reaction had been carried out. After removing the excess organic solution, the nano-composite membrane was left in an oven for a certain time (10–30 min) and temperature (20–80 °C) for evaporating n-hexane and further polymerization (post treatment). Finally, the nano-composite membrane was prepared, washed and stored in deionized water for determining the membrane performance.

Experimental design

It is important to note that response surface methodology (central composite design, CCD) was chosen for considering the composition effect of the independent variables (monomers concentrations, time and temperature) on the dependent variable (flux or removal efficiency), designing the experiments and data analysis (Yousefi *et al.* 2017). R software (Version 3.2.2) was used to analyze the results. Experimental design in this study was divided into two parts as follows:

Part 1: Experimental design for preparation of composite nanofiltration membranes.

Experiments with different TA and TMC concentrations, times and temperature were simultaneously conducted to include all possible permutations of the variables for the preparation of composite nanofiltration membranes in the CCD. A total of 44 experiments were conducted in this study, including 21 replicates at the center point. The coded values of the parameters were calculated using the following equation.

$$X_i = \frac{X_0 - X_1}{\Delta X} \tag{1}$$

where X_i is the coded value of the variable, X_1 the uncoded value of the test variable, and X_0 the uncoded value of the test variable at the center point.

$$Y = b_0 + \sum_{i=1}^{k} b_i X_i + \sum_{i=1}^{k} b_{ii} X_i^2 + \sum_{i=1}^{k-1} \sum_{i=1}^{k} b_{ij} X_i X_j + C \tag{2}$$

where Y is the dependent variable (NOM removal efficiency), b_0 is a constant value, b_i, b_{ii} and b_{ij} are regression coefficients for linear, second order and interaction effects, respectively, X_i and X_j are independent variables and C represents the prediction error.

The range of experimental and levels of the independent test variables is given in Table 1.

Part 2: Experimental design for optimization of the operational parameters for NOM removal.

Experiments with different NOM concentrations, time and pressure applied were simultaneously designed to include all possible permutations of the variables for NOM removal by prepared composite nanofiltration membranes in the CCD. A total of 63 experiments were conducted in this study, including 42 replicates at the center point. The coded values of the parameters were calculated using the above equation and experimental ranges and levels of the independent test variables are given in the Table 1.

Permeation and NOM rejection experiments

The separation performance of prepared nano-composite membranes were carried out using a stainless steel dead-end filtration system with a feed volume of 2 L and an effective membrane area of 9.6 cm^2. The water flux was calculated using the following equation.

$$J_w = \frac{V}{At} \tag{3}$$

where J_w is water flux ($L/m^2 \cdot h$), V is the volume of the permeated pure water (L), A is the effective area of the membrane (m^2) and t is the sampling time (h). Also, the

Table 1 | Experimental ranges and levels of the independent test variables for synthesis of membrane, and operational parameters

Synthesis of membrane

Parameters	Coded value	-α	−1	0	+1	+α
Tannic acid (mg/L)	X1	0	0.075	0.15	0.225	0.3
TMC (mg/L)	X2	0	0.075	0.15	0.225	0.3
Temperature (°C)	X3	20	35	50	65	80
Time (min)	X4	10	15	20	25	30
Operational parameters						
NOM (mg/L)	X1	5	6.91	12.5	18.09	20
Time (min)	X2	10	16.36	35	53.63	60
Pressure (bar)	X3	1	2	3	4	5

NOM removal efficiency was determined as:

$$R(\%) = 1 - \frac{C_p}{C_f} \times 100 \quad (4)$$

where R is the removal efficiency (%), C_p is the concentrations of NOM in the permeation solution (mg/L), C_f is the concentrations of NOM in the feed solution (mg/L).

Chemical stability of composite nanofiltration membranes

Certain concentrations of sodium hypochlorite and ethanol were prepared to evaluate the chemical stability of composite nanofiltration membranes. For determining the chemical stability, the composite nanofiltration membranes were taken out of the solutions and then the water fluxes and NOM removal were analyzed.

Fouling study of composite nanofiltration membrane

To evaluate the fouling mechanisms responsible in this study, the system was run as a dead-end condition and constant pressure (1 bar). Permeate volumes of water were measured at certain intervals and then the fouling of the mechanism was determined with the Herima empirical model.

RESULTS AND DISCUSSION

Membrane characteristics

Incorporation of hydrophilic polymers within PSf porous supports was characterized by ATR-FTIR. As presented in Figure 1, the spectrum of TA shows many sharp and strong peaks located at 1,748, 1,628, 1,443 and 1,309 cm^{-1}. Because the signal bands of carbonyl groups

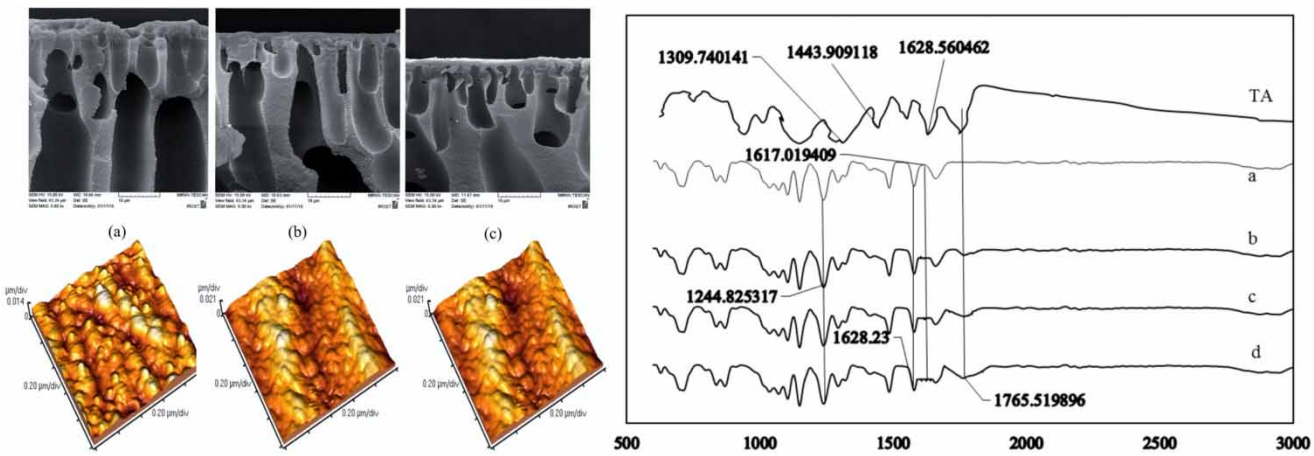

Figure 1 | Cross-sections FESEM micrographs and AFM images of synthesized nano-composite membranes. ATR-FTIR of tannic acid and synthesized membrane: TA, (a) PSf support, (b) TA: 0.1 TMC: 0.3, (c) TA: 0.3 TMC: 0.1, (d) TA: 0.3 TMC: 0.3.

Table 2 | Mean pore radius, water contact angle, porosity and pure water flux parameters of the prepared membranes

Membrane	TA (mg/L)	TMC (mg/L)	Mean pore radius (nm)	Contact angle (degree)	Porosity (%)	Flux (L/m²·h) at 1 bar	Surface zeta potential
PSf	–	–	22.3 ± 0.62	59.3 ± 2.1	73.1 ± 3.2	130 ± 5	−12.1 ± 1.3
1	0.1	0.3	19.2 ± 0.38	62.2 ± 2.25	61.3 ± 2.6	63.9 ± 2.3	−15.9 ± 0.9
2	0.3	0.1	14.6 ± 0.52	65.1 ± 1.6	48.5 ± 1.8	56.5 ± 2.1	−18.8 ± 2.5
3	0.3	0.3	12.3 ± 0.83	67.8 ± 1.3	42.6 ± 2.5	41.3 ± 3.2	−19.9 ± 3.2

(C = O (1,705–1,770 cm^{-1}) and etheric bands C-O (1,100–1,300 cm^{-1}), it can be presented that the TA contains aromatic esters (Mayra *et al.* 2012). According to the ATR-FTIR results, nano-composite membranes contain peaks at 1,765 cm^{-1} and 1,244 cm^{-1} that correspond to C = O and C–O (etheric group) bands, respectively. The signal bands at 1,748 and 1,628 cm^{-1} (H-O-H bending vibrations) appear in both TA and nano-composite spectra.

Surface SEM images and AFM for both the support membrane and nano-composite membranes are shown in Figure 1. According to these images, a denser structure and smoother active layer are apparent on the thin-film nano-composite in comparison with the ultrafiltration support membrane. This is morphological and structural evidence of potential to decrease the permeability. According to the AFM images, the roughness of membrane surfaces declines with increasing ratio of TA and TMC concentration. The depth of TA and TMC in the water interfacial zone is limited, therefore a thin and smooth layer is constructed on the porous ultrafiltration support.

Some characteristics of the nano-composite membrane are presented in Table 2. The contact angle increases with the increasing ratio of TA and TMC concentration, but with an increase of TMC concentration, the contact angle is slightly changed, which shows that the increasing TMC concentration made little contribution to the surface hydrophilicity (Zhao *et al.* 2014). In addition, the porosity of nano-composite membrane decreases as the concentration of monomers (TA in aqueous phase and TMC in organic phase) increases. In this phenomenon, the pores are blocked by high concentrations of monomers, which results in flux reduction (Wang *et al.* 2012). The results of monomer concentration effects on the membrane characteristics are consistent with similar work (Wu *et al.* 2013).

Preparation of composite nanofiltration membranes

The chemistry and the preparation conditions of the ultra-thin selective layer are the determining parameters for the

Table 3 | Observed and predicted values of NOM removal for the quadratic model

Run no.	X_1	X_2	X_3	X_4	R (%)	Predicted (%)	Run no.	X_1	X_2	X_3	X_4	R (%)	Predicted (%)
1	0.225	0.075	35	15	55.8	53.2	**23**	0.075	0.225	35	25	92.6	94.3
2	0.15	0.15	50	20	73.3	70.4	**24**	0.225	0.075	35	25	83.2	88.3
3	0.15	0.15	50	20	74.1	70.4	**25**	0.15	0.15	50	20	74.1	70.4
4	0.075	0.075	65	25	81.3	85.0	**26**	0.15	0.15	50	20	70.9	70.4
5	0.075	0.075	65	15	53.1	48.9	**27**	0.225	0.225	65	15	66.2	70.8
6	0.15	0.15	50	20	66.2	70.4	**28**	0.15	0.15	50	20	68.9	70.4
7	0.075	0.075	35	25	77.3	81.8	**29**	0.15	0.15	50	20	69.7	70.4
8	0.225	0.075	65	15	59.3	55.3	**30**	0.15	0.15	50	20	70.6	70.4
9	0.225	0.225	35	25	91.3	97.7	**31**	0.15	0	50	20	62.9	70.4
10	0.15	0.15	50	20	73.6	70.4	**32**	0.15	0.15	50	10	42.3	38.4
11	0.075	0.225	65	15	61.2	62.4	**33**	0.15	0.15	50	20	71.4	70.4
12	0.15	0.15	50	20	72.3	70.4	**34**	0.15	0.15	50	30	89.6	92.5
13	0.225	0.075	65	25	87.1	93.4	**35**	0.15	0.15	50	20	71.9	70.4
14	0.15	0.15	50	20	71.3	70.4	**36**	0	0.15	50	20	67.2	70.4
15	0.15	0.15	50	20	68.9	70.4	**37**	0.15	0.15	50	20	66.3	70.4
16	0.075	0.225	65	25	88.3	94.4	**38**	0.15	0.15	50	20	69.1	70.4
17	0.075	0.075	35	15	52.3	47.7	**39**	0.15	0.15	80	20	2.2	96.5
18	0.225	0.225	35	15	1.6	65.7	**40**	0.15	0.15	20	20	69.1	76.2
19	0.075	0.225	35	15	63.1	57.2	**41**	0.15	0.3	50	20	85.2	88.5
20	0.225	0.225	65	25	93.4	92.9	**42**	0.15	0.15	50	20	70.6	70.4
21	0.15	0.15	50	20	69.1	70.4	**43**	0.3	0.15	50	20	76.2	78.9
22	0.15	0.15	50	20	70.6	70.4	**44**	0.15	0.15	50	20	66.8	70.4

Table 4 | Analysis of variance (ANOVA) and regression analysis for the quadratic model for the preparation of membrane

Analysis of variance (ANOVA)

Model formula in RSM (X1, X2, X3, X4)	DF	Sum of squares	Mean squares	F-value	Probability (P)
FO	4	4785.3	196.32 19	0.6095	2.00×10^{-17}
TWI	6	30.8	5.13	0.8168	0.565845
PQ	4	146.0	36.5	5.8156	0.1457
Residuals	29	182.0	6.28	–	–
Lack of fit	10	72.3	7.23	1.2523	0.322
Pure error	19	109.7	5.77	–	–

Regression analysis for the quadratic model

Parameter	Coefficient estimate	Std error	t value	Pr(>|t|)
(Intercept)	70.485	0.56019	125.8228	$<2.2\times10^{-16}$
X_1	4.225	1.02277	4.131	0.00028
X_2	9.74167	1.02277	9.5248	1.97×10^{-10}
X_3	2.575	1.02277	2.5177	0.01759
X_4	26.04167	1.02277	25.462	$<2.2\times10^{-16}$
X_2^2	4.63583	1.71142	2.7088	0.01121
X_3^2	5.23583	1.71142	3.0594	0.00474
X_4^2	−3.46417	1.71142	−2.0242	0.05225

F-statistic: 56.47 on 14 and 29, DF, p-value: $<2.00\times10^{-16}$, Multiple R^2: 0.9646, Adjusted R^2: 0.9475, Predicted R^2: 0.9347, Lack of fit: 0.322061.

evaluation of the performance of the nano-composite membrane. So, the optimal performance characteristics could be determined by investigating the effective parameters on the preparation conditions of nano-composite membrane. Experimental and predicted values of NOM removal, analysis of variance (ANOVA) for the preparation of membrane and regression analysis for the quadratic model are presented in Tables 3 and 4, respectively. The predicted data were best fitted with the experimental data ($R^2 > 0.96$) which shows that the quadratic model is in good agreement for predicting the preparation of nano-composite membranes. Based on the results, the effect of all parameters on the membrane preparation was significant, but the effect of monomer concentrations and time (post treatment) were significantly higher than the temperature.

It could be observed that rejection was significantly increased with increasing in the monomer concentration. At first, increases in NOM removal was slow; at high concentration of monomers, removal of NOM sharply increased with further increase of monomer concentrations. These events can be related to the reaction between TA and TMC in the interfacial zone. The results of monomer concentrations disclosed that the phenolic groups of TA chemically created a cross-link with TMC, while TMC bonded with triacyl chloride functional groups on the support membrane. The high cross-linking reaction extent between aqueous phase and organic phase led to lower pore densities in the thin films.

The effect of reaction time (post treatment) on the preparation of composite nanofiltration membranes revealed that the reaction time has a remarkable effect on the interfacial polymerization (Figure 2). It can clearly be seen that a long reaction time post treatment can alleviate the degree of polymerization on the support membrane (PSf).

To obtain the optimal performance characteristics of nano-composite membrane preparation using the model equation predicted by RSM, the Solver 'Add-ins' was used. The predicted optimum operational conditions were a TA concentration of 0.27 g/L, TMC concentration of 0.22 g/L, reaction time of 68.29 min and temperature of 25.53 °C, and the maximum removal efficiency was estimated to be 98.65%. Also, additional laboratory experiments were used to confirm the validity of the results predicted by the model.

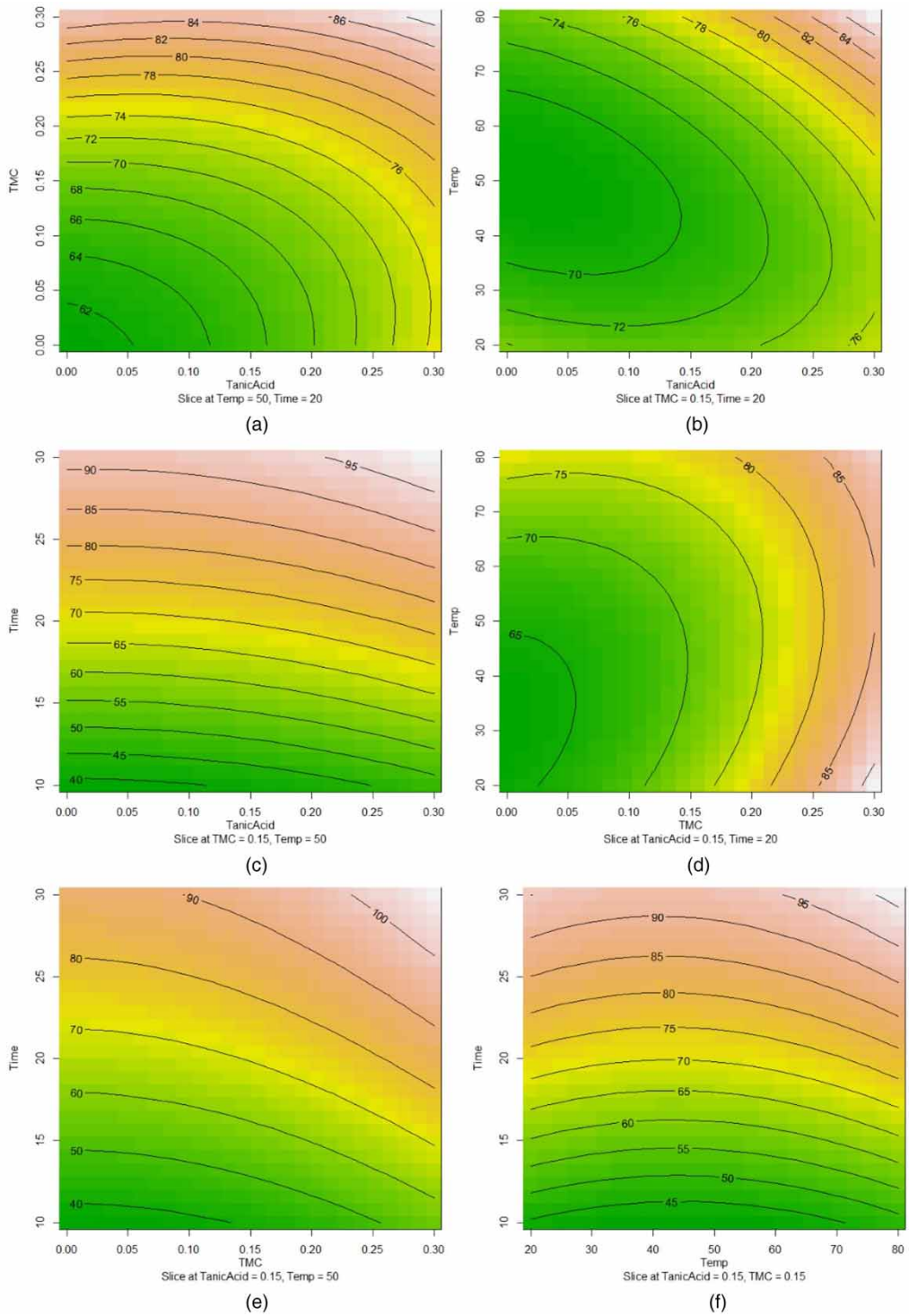

Figure 2 | Contour plots of NOM removal efficiency as a function of independent variables: (a) TA and TMC, (b) TA and temperature, (c) TA and time, (d) TMC and temperature, (e) TMC and time, and (f) temperature and time.

Permeation and NOM rejection experiments

The experimental and predicted values for preparation of nano-composite membranes for NOM removal (%) (Table 5) obtained from the quadratic model is shown in Table 6. As shown in Table 6, the predicted data were best fitted with the experimental data ($R^2 > 0.93$) which indicates the quadratic model is a good accordance with

Table 5 | Observed and predicted values of NOM removal for the quadratic model

Run no.	X_1	X_2	X_3	R (%)	Predicted (%)	Run no.	X_1	X_2	X_3	R (%)	Predicted (%)
1	12.5	35	1	77.54	69.25	**33**	6.90	16.3	5	91.39	91.59
2	12.5	35	3	72.04	72.06	**34**	12.5	35	1	74.55	69.25
3	12.5	35	5	68.93	74.87	**35**	12.5	35	3	72.04	72.06
4	12.5	35	1	74.13	69.25	**36**	12.5	35	5	68.89	74.87
5	12.5	35	3	71.73	72.06	**37**	5	35	1	96.49	88.21
6	12.5	35	5	68.62	74.87	**38**	5	35	3	92.41	92.60
7	12.5	35	1	74.91	69.25	**39**	5	35	5	87.69	97.00
8	12.5	35	3	44.72	72.06	**40**	12.5	35	1	74.01	72.06
9	12.5	35	5	65.09	74.87	**41**	12.5	35	3	71.63	74.87
10	12.5	35	1	73.93	69.25	**42**	12.5	35	5	68.36	69.25
11	12.5	35	3	71.46	72.06	**43**	12.5	10	1	81.43	77.16
12	12.5	35	5	68.38	74.87	**44**	12.5	10	3	77.29	78.02
13	18.09	53.6	1	54.13	44.91	**45**	12.5	10	5	76.12	76.31
14	18.09	53.6	3	57.85	47.99	**46**	12.5	60	1	60.76	56.35
15	18.09	53.6	5	44.47	51.07	**47**	12.5	60	3	58.47	61.11
16	12.5	35	1	74.61	69.25	**48**	12.5	60	5	51.24	51.59
17	12.5	35	3	72.12	72.06	**49**	20	35	1	52.07	51.52
18	12.5	35	5	69.06	74.87	**50**	20	35	3	51.16	52.74
19	18.09	16.3	1	59.22	44.91	**51**	20	35	5	48.51	50.30
20	18.09	16.3	3	59.37	47.99	**52**	12.5	35	1	81.52	72.06
21	18.09	16.3	5	71.21	51.07	**53**	12.5	35	3	72.62	74.87
22	12.5	35	1	74.71	69.25	**54**	12.5	35	5	63.54	69.25
23	12.5	35	3	72.25	72.06	**55**	12.5	35	1	77.55	72.06
24	12.5	35	5	63.24	74.87	**56**	12.5	35	3	73.21	74.87
25	6.9	53.6	1	79.62	69.27	**57**	12.5	35	5	68.26	69.25
26	6.9	53.6	3	74.47	74.72	**58**	12.5	35	1	74.84	72.06
27	6.9	53.6	5	67.72	80.17	**59**	12.5	35	3	72.44	74.87
28	12.5	35	1	74.51	69.25	**60**	12.5	35	5	61.61	69.25
29	12.5	35	3	71.98	72.06	**61**	12.5	35	1	74.21	72.06
30	12.5	35	5	68.82	74.87	**62**	12.5	35	3	71.74	74.87
31	6.90	16.3	1	96.45	91.59	**63**	12.5	35	5	68.65	69.25
32	6.90	16.3	3	94.23	94.13						

predicting the value of NOM removal by nano-composite membranes.

The results of variance analysis (ANOVA) for NOM removal are illustrated in Table 6. Low *P*-value (<0.034), high F-value, high R^2 (>0.93) and insignificant lack of fit (0.18) showed that the quadratic model was significant for NOM removal using the nano-composite membrane. Also, high R^2 values and its good agreement with R^2_{adj} indicates a high correlation between the experimental and predicted values. In addition, the results showed that all variables (X_1: NOM concentration; X_2: time and X_3: applied pressure) had a significant effect on NOM removal. The maximum F-value was for NOM concentration (223.7) which indicates that the NOM concentration is the most effective parameter for NOM removal, while the applied pressure is the least effective parameter. Also, contour plots of NOM removal efficiency as the function of independent variables are illustrated in Figure 3.

Table 6 | Analysis of variance (ANOVA) and regression analysis for the quadratic model for the operational parameters

Analysis of variance (ANOVA)

Model formula in RSM (X1, X2, X3, X4)	DF	Sum of squares	Mean squares	F-value	Probability (P)
FO	3	6501.6	2167.21	223.7129	$<2.2\times10^{-16}$
TWI	3	182.6	60.86	6.2828	0.0009967
PQ	3	81.2	27.08	2.7956	0.0490435
Residuals	53	513.8	9.69	–	–
Lack of fit	17	207.3	12.20	1.4345	0.1774642
Pure error	36	306.1	8.50	–	–

Regression analysis for the quadratic model

Parameter	Coefficient estimate	Std. error	t value	Pr(>|t|)
(Intercept)	72.05621	0.74533	96.6772	$<2.20\times10^{-16}$
X_1	−19.1321	0.87453	−21.8771	$<2.20\times10^{-16}$
X_2	−10.5902	0.87453	−12.1096	$<2.20\times10^{-16}$
X_3	−3.25333	0.48026	−6.774	1.04×10^{-8}
$X_1\times X_2$	4.0365	1.61729	2.4958	0.015712
$X_1\times X_3$	2.32317	1.07107	2.169	0.034588
$X_2\times X_3$	−3.01325	1.07107	−2.8133	0.006864
X_2^2	−3.31457	1.17894	−2.8115	0.006898

F-statistic: 77.6 on 9 and 53 DF, p-value: $<2.2\times10^{-16}$, Multiple R^2:0.9295, Adjusted R^2: 0.9175, Predicted R^2: 0.9126, Lack of fit: 0.1774642.

It has been mentioned that the RSM results need to be analyzed through the optimization process. The criteria were maximum for NOM removal, NOM concentration (5–20 mg/L), time (10–60 min) and applied pressure (1–5 bar). In the optimum conditions, all parameters simultaneously met the predicted desirable criteria. According to the assumptions, the predicted optimum operational conditions were: NOM concentration of 6.429 mg/L; time of 10.931 min and applied pressure of 1.039 bar, and the maximum removal efficiency was estimated to be 98.86%. Also, additional laboratory experiments were conducted to confirm the validity of the results predicted by the model.

Fouling study of composite nanofiltration membrane

Hermia's blocking laws is one of the most popular models can be applied to determine the fouling mechanism in membrane science. This empirical model was illustrated as the following equation:

$$\frac{d^2t}{dv^2} = k\left(\frac{dt}{dv}\right)^n \tag{5}$$

where v is volume (L), t is time (s), k is the blocking law filtration coefficient (unit depends on n) and n is the blocking law filtration exponent (dimensionless). n expresses the fouling regime. In this models, the n values indicate different modes of fouling: cake filtration ($n=0$), pore sealing with superposition ($n=1$), internal pore constriction ($n=1.5$) and pore sealing ($n=2$) (Crittenden *et al.* 2012). In fouling analysis of the filtration process, a combination of mechanisms may occur. According to the result, the fouling mechanism is internal pore constriction ($n=1.56$) (Figure 4), which shows that the molecular sizes of the foulants are larger than the pore size of nano-composite membranes and thus could not penetrate into the pores and therefore caused surface fouling. Hydroxyl groups on the nano-composite membrane prepared were responsible for the antifouling properties of the membrane, because they prevent contact between foulant and membrane surfaces, as mentioned above.

Chemical stability of the composite nanofiltration membranes

The chemical stability of a membrane is very important for operating the membrane process. It is found that chloride

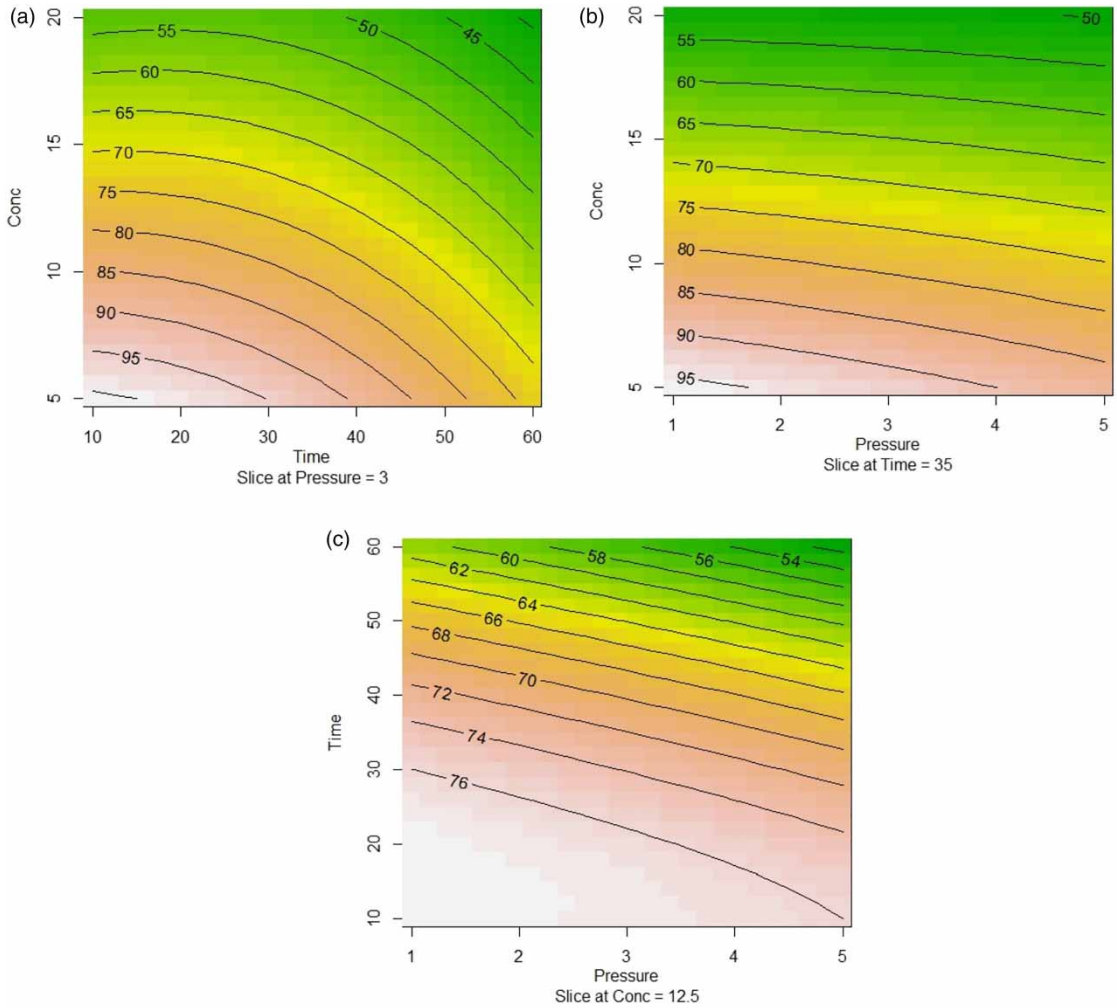

Figure 3 | Contour plots of NOM removal efficiency as the function of independent variables: (a) concentration of NOM and time, (b) concentration and pressure, and (c) time and pressure.

causes the destruction or detachment of the separation layer, decreasing the separation performance and finally shortening the lifespan of the composite nanofiltration membrane (Minhas *et al.* 2013).

Figure 4 shows the result of chemical stability of nano-composite membrane and the effect of ethanol and sodium hypochlorite concentrations on the nano-composite performance.

It is clear that the NOM rejections were sustained at more than 80% after eight days and the water fluxes had increased from 37.6 to 72.5 L/m^2·h and 37.6 to 61.2 L/m^2·h for NaOCl and ethanol, respectively. It was found that the rejection of NOM presented a slight variation in ethanol and n-hexane fluxes up to eight days which shows good chemical stability of the membrane (Yousefi *et al.* 2017). The nano-composite nanofiltration membranes were resistant to organic and chemical reagents because of the carbonyl groups and carbonyl etheric bands (C = O and C-O) which are much more stable to oxidation. Therefore, the potential applications of the synthesized nano-composite membranes can enhance water treatment (Yousefi *et al.* 2017).

CONCLUSIONS

In this study, nano-composite synthesis by TA and TMC with interfacial polymerization, structural properties, NOM rejection, fouling mechanism, antifouling properties and chemical stability have been discussed. Nano-composite membranes were more hydrophilic. Interfacial polymerization led to higher NOM rejection. Increase in applied pressure enhanced the pure water and solute permeability. According to the results, the fouling mechanism is internal pore constriction ($n = 1.56$). The potential applications of

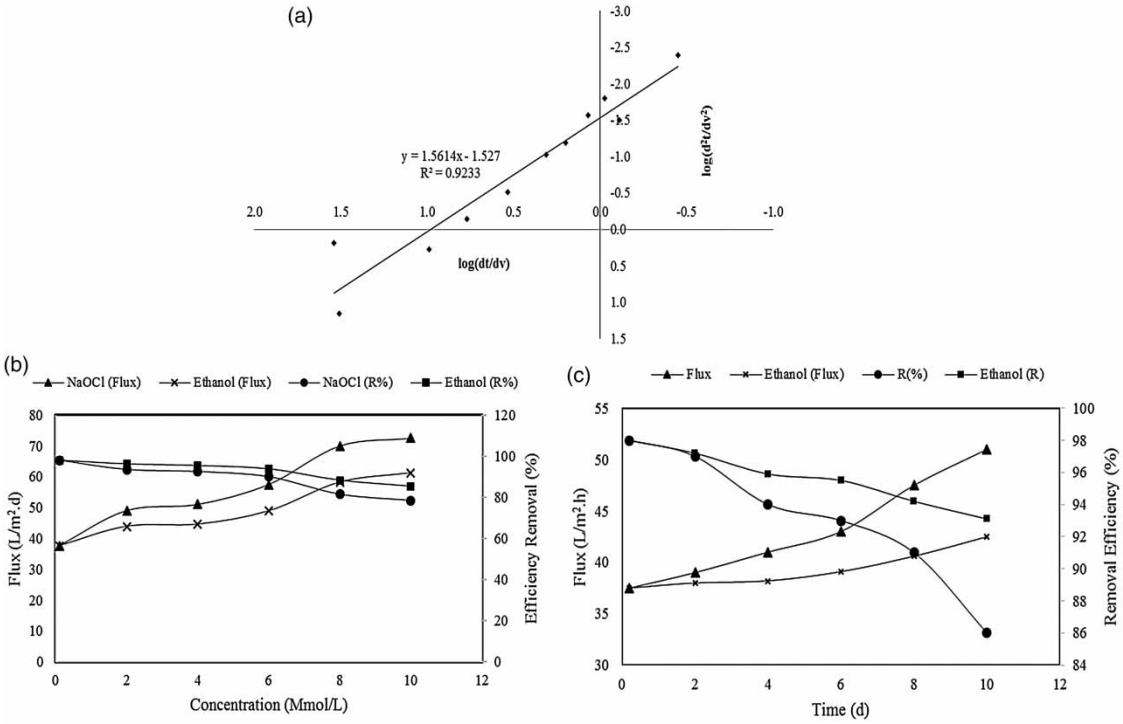

Figure 4 | (a) Fouling analysis for HA filtration of nano-composite membrane (HA: 10 ± 0.2 mg/L, pH: 7 ± 0.15, 1 bar) (b) The effect of ethanol and sodium hypochlorite concentrations (immersion time: 8 days, 2 bar) and (c) immersion time (2 Mmol/L sodium hypochlorite and ethanol solution, 2 bar) on the water fluxes and NOM removal.

the nano-composite membranes can enhance water treatment.

ACKNOWLEDGEMENTS

This research was part of a Ph.D. dissertation and was financially supported by a grant (Project No. 94-04-46-28520) from the Center for Water Quality Research, Institute for Environmental Research, Tehran University of Medical Sciences, Tehran, Iran. The authors would like to thank the Department of Environmental Health Engineering, School of Public Health, Tehran University of Medical Sciences for their collaboration.

REFERENCES

Ashrafi, S. D., Rezaei, S., Forootanfar, H., Mahvi, A. H. & Faramarzi, M. A. 2013 The enzymatic decolorization and detoxification of synthetic dyes by the laccase from a soil-isolated ascomycete, paraconiothyrium variabile. *International Biodeterioration & Biodegradation* **85**, 173–181.

Ashrafi, S., Kamani, H., Soheil Arezomand, H., Yousefi, N. & Mahvi, A. 2016 Optimization and modeling of process variables for adsorption of basic blue 41 on NaOH-modified rice husk using response surface methodology. *Desalination and Water Treatment* **57** (30), 14051–9.

Crittenden, J. C., Trussell, R. R., Hand, D. W., Howe, K. J. & Tchobanoglous, G. 2012 *MWH's Water Treatment: Principles and Design*. John Wiley & Sons, New Jersey, USA.

Dehghani, M. H., Mesdaghinia, A. R., Nasseri, S., Mahvi, A. H. & Azam, K. 2008 Application of SCR technology for degradation of reactive yellow dye in aqueous solution. *Water Qual. Res. J. Can.* **43** (2/3), 1–10.

Gholami-Borujeni, F., Mahvi, A. H., Naseri, S., Faramarzi, M. A., Nabizadeh, R. & Alimohammadi, M. 2011a Application of immobilized horseradish peroxidase for removal and detoxification of azo dye from aqueous solution. *Res. J. Chem. Environ.* **15** (2), 217–222.

Gholami-Borujeni, F., Mahvi, A. H., Nasseri, S., Faramarzi, M. A., Nabizadeh, R. & Alimohammadi, M. 2011b Enzymatic treatment and detoxification of acid orange 7 from textile wastewater. *Applied Biochemistry and Biotechnology* **165** (5–6), 1274–1284.

Habuda-Stanić, M., Romić, Ž., Nujić, M., Santo, V. & Kuvedžić, Z. 2013 Effects of activated carbon types on NOM removal effect from natural waters. *Technologica Acta* **29**, 29–38.

Jafari, A., Mahvi, A. H., Nasseri, S., Rashidi, A., Nabizadeh, R. & Rezaee, R. 2015 Ultrafiltration of natural organic matter from water by vertically aligned carbon nanotube membrane. *Journal of Environmental Health Science and Engineering* **13** (1), 1.

Korikov, A., Kosaraju, P. & Sirkar, K. 2006 Interfacially polymerized hydrophilic microporous thin film composite

membranes on porous polypropylene hollow fibers and flat films. *Journal of Membrane Science* **279**, 588–600.

Li, L., Zhang, S. & Zhang, X. 2009 Preparation and characterization of poly(piperazineamide) composite nanofiltration membrane by interfacial polymerization of 3,3,5,5-biphenyl tetraacyl chloride and piperazine. *Journal of Membrane Science* **335**, 133–139.

Mahvi, A., Gholami, F. & Nazmara, S. 2008 Cadmium biosorption from wastewater by Ulmus leaves and their ash. *European Journal of Scientific Research* **23** (2), 197–203.

Mahvi, A., Ghanbarian, M., Nasseri, S. & Khairi, A. 2009 Mineralization and discoloration of textile wastewater by tio2 nanoparticles. *Desalination* **239** (1–3), 309–316.

Mahvi, A. H., Malakootian, M., Fatehizadeh, A. & Ehrampoush, M. H. 2011 Nitrate removal from aqueous solutions by nanofiltration. *Desalination and Water Treatment* **29** (1–3), 326–330.

Malakootian, M., Fatehizadeh, A. & Yousefi, N. 2011 Evaluating the effectiveness of modified pumice in fluoride removal from water. *Asian Journal of Chemistry* **23** (8), 3691.

Malakootian, M., Yousefi, N., Fatehizadeh, A., Van Ginkel, S. W., Ghorbani, M., Rahimi, S. & Ahmadian, M. 2015 Nickel (II) removal from industrial plating effluent by Fenton process. *Environmental Engineering and Management Journal* **14** (4), 837–842.

Maleki, A., Mahvi, A. H., Ebrahimi, R. & Zandsalimi, Y. 2010 Study of photochemical and sonochemical processes efficiency for degradation of dyes in aqueous solution. *Korean Journal of Chemical Engineering* **27** (6), 1805–1810.

Mayra, A., Castro, P. & Rodríguez, H. 2012 Study by infrared spectroscopy and thermogravimetric analysis of tannins and tannic acid. *Rev. Latinoamer. Quím* **39** (3), 107–112.

Minhas, F. T., Memon, S., Bhanger, M., Iqbal, N. & Mujahid, M. 2013 Solvent resistant thin film composite nanofiltration membrane: characterization and permeation study. *Applied Surface Science* **282**, 887–897.

Rezaee, R., Maleki, A., Jafari, A., Mazloomi, S., Zandsalimi, Y. & Mahvi, A. H. 2014 Application of response surface methodology for optimization of natural organic matter degradation by UV/H_2O_2 advanced oxidation process. *Journal of Environmental Health Science and Engineering* **12** (1), 1.

Seman, M. A., Kei, L. & Yusoff, M. 2015 Synthesis and performance of polyamide forward osmosis membrane for natural organic matter (NOM) removal. *Agricultural and Biosystems Engineering* **2** (1), 160–163.

Shirmardi, M., Mesdaghinia, A., Mahvi, A. H., Nasseri, S. & Nabizadeh, R. 2012 Kinetics and equilibrium studies on adsorption of acid red 18 (Azo-Dye) using multiwall carbon nanotubes (MWCNTs) from aqueous solution. *Journal of Chemistry* **9** (4), 2371–2383.

Wang, Z., Yu, H., Xia, J., Zhang, F., Li, F., Xia, Y. & Li, Y. 2012 Novel GO-blended PVDF ultrafiltration membranes. *Desalination* **299**, 50–54.

Wu, H., Tang, B. & Wu, P. 2013 Optimization, characterization and nanofiltration properties test of MWNTs/polyester thin film nanocomposite membrane. *Journal of Membrane Science* **428**, 425–433.

Yousefi, N., Fatehizedeh, A., Ghadiri, K., Mirzaei, N., Ashrafi, S. D. & Mahvi, A. H. 2016 Application of nanofilter in removal of phosphate, fluoride and nitrite from groundwater. *Desalination and Water Treatment* **57** (25), 11782–8.

Yousefi, N., Nabizadeh, R., Nasseri, S., Khoobi, M., Nazmara, S. & Mahvi, A. H. 2017 Decolorization of direct blue 71 solutions using tannic acid/polysulfone thin film nanofiltration composite membrane; preparation, optimization and characterization of anti-fouling. *Korean Journal of Chemical Engineering* **34** (8), 2342–2353.

Zhao, Y., Hu, X., Jiang, B. & Li, L. 2014 Optimization of the operational parameters for desalination with response surface methodology during a capacitive deionization process. *Desalination* **336**, 64–71.

First received 31 May 2017; accepted in revised form 12 January 2018. Available online 24 January 2018